

# Toward Exascale AI for Science: A Scalable AI Skill for Autonomous Microkinetics Discovery

Ken-ichi Nomura  
knomura@usc.edu  
University of Southern California  
Los Angeles, CA, USA

William Dawson  
william.dawson@riken.jp  
RIKEN R-CCS  
Kobe, Japan

Nabankur Dasgupta  
ndasgupt@usc.edu  
University of Southern California  
Los Angeles, CA, USA

Taufeq Mohammed Razakh  
razakh@usc.edu  
University of Southern California  
Los Angeles, CA, USA

Thomas Linker  
tlinker@slac.stanford.edu  
SLAC National Accelerator  
Laboratory  
Menlo Park, CA, USA

Kai Ito  
ki\_790@usc.edu  
Kumamoto University  
Kumamoto, Japan

Aiichiro Nakano  
anakano@usc.edu  
University of Southern California  
Los Angeles, CA, USA

## Abstract

We present a scalable AI-driven framework that advances autonomous scientific discovery by combining agentic workflow automation, high-performance computing, and scientific surrogate models. Using microkinetics discovery as a testbed, the work demonstrates how AI can reduce expert intervention, recover from failed simulations, and systematically evaluate surrogate model reliability. This study shows how AI skills can transform complex domain workflows into robust, scalable capabilities for next-generation materials research.

## CCS Concepts

• Applied computing → Engineering; • Computing methodologies → Multi-agent systems; *Parallel algorithms*.

### ACM Reference Format:

Ken-ichi Nomura, William Dawson, Nabankur Dasgupta, Taufeq Mohammed Razakh, Thomas Linker, Kai Ito, and Aiichiro Nakano. 2026. Toward Exascale AI for Science: A Scalable AI Skill for Autonomous Microkinetics Discovery. In *Proceedings of ACM AI Leadership Summit 2026 (AI Summit '26)*. ACM, New York, NY, USA, 5 pages. <https://doi.org/XXXXXXXX.XXXXXXX>

## 1 Introduction

A grand challenge in science is to understand complex materials from first principles – a challenge best addressed by multiscale simulation [29]. Today, the-state-of-the-art (SOTA) is combined deployment of multi-exaflop quantum mechanical (QM) simulations

with surrogate foundation models [36, 17], a formidable modeling task at the intersection of high-performance computing (HPC), AI, and applied science. A prototypical use case is reaction kinetics of complex material structures [45, 22], a regime where even small scale QM simulations are laborious and the establishment of robust foundation models remains unrealized.

Agentic AI – characterized by autonomy, planning, and task execution – promises to vault materials research over these technical barriers through the automation of workflows that once only humans could manage. Agents deployed for scientific tasks integrate domain specific knowledge and tools for long term memory [27, 16], information retrieval [27, 16], and interaction with external software [43, 13] or resources [7, 25]. Composable augmentation is typically achieved today through two means: the Model Context Protocol (MCP) [2] and agent skills [1, 42]. Skills in particular have gained traction as a lightweight abstraction layer to teach Large Language Models (LLMs) domain-specific and procedural knowledge. Embedding these capabilities into agent harnesses transforms general-purpose frameworks (e.g., OpenClaw [39], NemoClaw [31]) into “AI scientists.” With the rapid adoption of automated AI workflows across the scientific community [35, 7], ensuring their consistency, reproducibility, and reliability has become an urgent priority [24].

Agent tools and skills to leverage HPC resources would accelerate materials research through three complementary pillars: agentic automation, materials-specific surrogate models, and large-scale simulations on exascale computing infrastructure. Agents backed by open models running on national supercomputing infrastructure would in turn manage simulations on the same or complementary infrastructure. Unfortunately, domain-specific frameworks – particularly incorporating HPC [9] – able to robustly perform simulations despite the sycophantic nature of LLMs [26], remain in their infancy. In this work, we realize this vision as an HPC centric agent able to perform reaction kinetics simulations at scale, and evaluate its performance for comparing different universal models for material properties.

Permission to make digital or hard copies of all or part of this work for personal or classroom use is granted without fee provided that copies are not made or distributed for profit or commercial advantage and that copies bear this notice and the full citation on the first page. Copyrights for components of this work owned by others than the author(s) must be honored. Abstracting with credit is permitted. To copy otherwise, or republish, to post on servers or to redistribute to lists, requires prior specific permission and/or a fee. Request permissions from [permissions@acm.org](mailto:permissions@acm.org).

*AI Summit '26, Atlanta, GA*

© 2026 Copyright held by the owner/author(s). Publication rights licensed to ACM.  
ACM ISBN 978-1-4503-XXXX-X/2018/06  
<https://doi.org/XXXXXXXX.XXXXXXX>

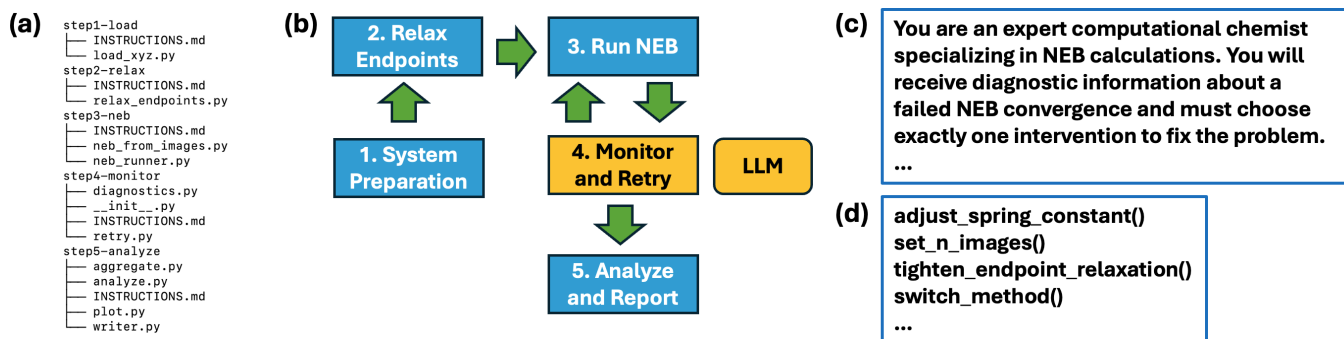


**Figure 1: Design of NEB skill.** (a) Directory and file organization of the five key steps. (b) Skill flowchart. A user initiates the skill by providing reactant and product coordinates. Locally executed tasks are indicated by blue boxes, while yellow boxes indicate HPC inference by LLM. During the *Monitor and Retry* step, an agent is given system task (c), and decides strategies (d) to improve the success rate of NEB calculation.

## 2 Methodology

### 2.1 Skill Design

To explore the potential of agent skills, we have developed “nebskill” [30] for Nudged Elastic Band (NEB) [21, 18] calculation. NEB searches for the minimum energy pathway (MEP) between a reactant and product to determine the transition state and activation energy of a chemical reaction. Although the methodology is well established, NEB calculations are highly sensitive to the choice of parameters and the system of interest. This dependency often turns conceptually simple work into labor-intensive jobs that take days, if not weeks. Hence, agentic automation offers the promise of increasing scientific productivity for these studies. Though fully autonomous AI scientists have garnered significant attention [24], their widespread adoption remains hindered by the lack of one-size-fits-all solutions; we therefore adopt a co-scientist approach for the “nebskill”, emphasizing immediate, practical value for a community increasingly exploring agentic workflows.

Figure 1 (a) shows the organization of directories and files. The top directory contains SKILL.md markdown file and each subdirectory contains another markdown file INSTRUCTIONS.md. This allows the agent to process the skill as it progresses, as well as to divide the entire task into smaller subtasks to reduce the chance of context rot [20]. The five key steps of the skill are shown below:

- **Step1:** Initialization: setup environment (e.g., download MLIP models, verify reactant and product coordinates).
- **Step2:** Relax reactant and product configurations.
- **Step3:** Interpolate between the reactant and product, then run a two phase calculation – standard NEB followed by Climbing-Image (CI) NEB.
- **Step4:** Monitoring and failure recovery. Upon a calculation failure, LLM diagnoses the cause and proposes a new set of parameters (e.g., number of NEB images, spring constant).
- **Step5:** Analysis and report. Methods from domain experts are applied to converged calculations to verify the chemistry.

When a job fails, the agent diagnoses the cause and proposes a new job to try (Step 4) following the ReAct (reasoning and acting) [44] approach. Based on observations from the failed job, the

agent makes a decision on whether to exploit accumulated knowledge of the ongoing campaign (e.g., slightly update the value of spring constant) or to explorer a new strategy (e.g., change the interpolation scheme from linear to spline). In this work, we use ALCF (Argonne Leadership Computing Facility) Inference Endpoint, through which we access high-throughput AI services at scale. The API is called with a system prompt (Fig. 1c) along with the current NEB parameters and the diagnosis to propose a next strategy (Fig. 1d). Building on our previous integration of agents with supercomputer Fugaku [9], we performed scalability tests on the Perlmutter cluster at the National Energy Research Scientific Computing Center (NERSC). Under the US-Japan Genesis partnership, we plan to use these globally distributed supercomputers as a single metacomputer to perform grand challenge AI-simulation workflows otherwise impossible, leveraging our previous US-Japan metacomputing paradigm [41].

### 2.2 Surrogate Models and Dataset

Equivariant networks for interatomic potential encode atomic environments by expanding interatomic displacements into spherical harmonics, yielding internal features that transform as proper geometric tensors under rotation [10, 3]. By enforcing equivariance throughout network architecture, the model does not need to relearn the same physics in arbitrarily rotated orientations, yielding substantially better data efficiency, smoother and more physically consistent force/stress predictions, and improved extrapolation to geometries and compositions outside the training distribution.

While many network architectures have been proposed to date [37], NequIP [5] and MACE [4] are widely used equivariant MLIP models based on message-passing scheme to build multi-body correlations over successive graph convolutions. Allegro model [28] employs a strictly local feature approach where pairwise equivariant feature tensors are iteratively refined through tensor products with neighboring pairs sharing a central atom, preserving algorithmic scalability without sacrificing expressivity.

In this work, the agent examines a number of SOTA pretrained universal MLIP models as a surrogate of graphite surface microkinetics. We evaluate over ten SOTA MLIP models to find the best

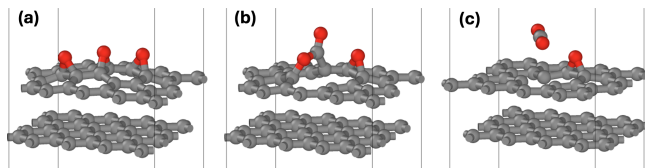


**Figure 2: (a) Atomic configurations of reactant, (b) transition state, and (c) product obtained with ab-initio calculation. Red spheres for oxygen and gray ones for carbon atoms, respectively. The first step of NEB calculation is to smoothly interpolate the reactant and product configurations and generate an initial guess of intermediate states (i.e. NEB images).**

surrogate model that matches with a given ground truth result. Figure 2 presents the atomic configurations during the sublimation of  $\text{CO}_2$  from graphite surface obtained by ab-initio quantum mechanics (QM) calculation and used to evaluate the developed AI skill.

**QM calculation:** We perform adiabatic quantum molecular dynamics simulations using the QXMD software [38]. A QMD simulation [8, 33] follows the trajectory of all atoms, while calculating interatomic forces quantum mechanically from first principles within the framework of density functional theory (DFT) [19]. The electronic states are calculated using the projector-augmented wave (PAW) method [6], where projector functions are generated for  $2s^22p^2$  for C,  $2s^22p^4$  for O atoms. The generalized gradient approximation (GGA) is used for the exchange-correlation functional [34] and DFT-D2 for the dispersion correction [15]. The plane-wave cutoff energies are set to 30 Ry for the wavefunction and 300 Ry for the electron density in all calculations. We used  $4 \times 4 \times 1$   $k$ -points for Brillouin zone sampling.

**Graphite model:** A graphite consists of two graphene layers. The graphene sheet consisting of 4 unit cells with a lattice constant of 1.43 Å. To prevent interaction between periodic images along the  $z$  direction due to the periodic boundary conditions, a vacuum layer of thickness 14 Å is introduced along the  $z$  axis. The supercell is orthorhombic with dimensions of  $8.38 \times 9.91 \times 17.7$  Å<sup>3</sup>.

## 3 Results

### 3.1 Reaction Coordinate and Activation Energy

Fig. 3 presents the energy profiles obtained by SOTA MLIP models together with DFT calculations (black) as the ground truth. While quantitative comparisons may not be straightforward without fine-tuning, some of the MLIP models agree reasonably well with the ground truth calculation. For example, among all models, mace-mp-l shows the closest activation energy, while the energy curve of nequip-oam and allegro-oam closely follows the DFT result. In terms of reaction mechanism, all models predict the lactone-mediated  $\text{CO}_2$  sublimation mechanism that was also verified by other QM calculations [40, 23].

### 3.2 Scalability Test

To maximize parallel efficiency and improve time-to-solution, our agent skill employs two-dimensional parallelism over the MLIP model and NEB images. While the concurrency of model parallelism

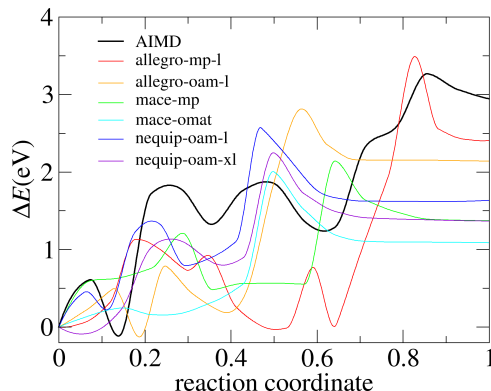


**Figure 3: Activation energy along the reaction coordinate predicted by pretrained MLIP models compared against ground truth DFT calculations (black). The horizontal axis is normalized by the total number of NEB images.**

differs case by case, typically 5 to 10 MLIP models are evaluated simultaneously to improve the statistics. Since model parallelism are loosely coupled, each MLIP evaluation is distributed over different nodes. In contrast, parallelization over NEB images is tightly coupled due to frequent atomic force exchanges. To minimize communication latency, the NEB images (typically 10 to 30) are distributed across the GPUs of a single node in a round-robin fashion to accelerate the overall calculation.

We have performed scalability test of the AI skill on the Department of Energy (DOE) leadership computing facilities, Perlmutter cluster at NERSC and the Inference Endpoint at ALCF. The Perlmutter cluster based on HPE Cray system consists of 3,072 CPU and 1,792 GPU nodes. Each GPU node hosts four NVIDIA A100 GPUs. The ALCF Inference Endpoint comprises of Sophia (NVIDIA DGX A100) and Metis (SambaNova) and offers DOE scientists high-throughput, low-latency AI inference capabilities. Currently dozens of open foundation models are supported, including Google Gemma [14], Meta LLaMA [11], and OpenAI GPT-OSS [32].

Table 1 shows the runtime improvement from baseline. All measurements were done on Perlmutter at NERSC. While the scalability performance is impacted by many external factors, e.g. filesystem access, we have achieved nearly perfect speed up using a factor of 3.75 $\times$  speed up on four GPU nodes with nearly perfect parallel efficiency.

**Table 1: Scalability of distributed NEB computing**

Node	GPUs	wallclock (min)	speed up
1	4	116.9	1.0 (baseline)
2	8	84.3	1.39
3	12	61.0	1.92
4	16	32.1	3.75

### 3.3 Failure and Retry Analysis

Because NEB calculation explores the energy landscape of target system, its success is highly dependent on researchers' knowledge

and familiarity of the target system. Researchers often figure out an optimal configuration after time-consuming try-and-error efforts. Therefore, investigating the cause of NEB calculation failures, retry strategies, and its cost would provide useful insights of the system and actionable strategies for improvement. Here, we present case study on failed NEB jobs and the robustness of MLIP model predictions.

We have identified 54 jobs in this study that failed in the first attempt but successfully converged at the end. We called them "resilient" NEB job. Of all, 51 jobs were found "image collapse" where the distance between each NEB image became too close, most likely attributed to the value of spring constant being too low. The remaining three jobs are "kinking" in the energy profile, exhibiting discontinuities or being very noisy.

**Table 2: Five representative NEB calculations that successfully converged after several retries by agent. Used MLIP model, attempted retries (from top to bottom), the number of consumed tokens, and communication time with ALCF Inference Endpoint are shown respectively.**

MLIP	retry	tokens	comm. (s)
mace-mp	adjust spring adjust spring set N images adjust spring	6642	23.17
allegro-oam-l	adjust spring	1595	14.48
pet-omat	adjust spring adjust spring set N images	4686	19.43
pet-omat	adjust spring adjust spring	3305	11.03
allegro-oam-l	adjust spring	1593	14.41

Table 2 presents five representative cases out of the resilient job pool. The default strategy taken by agent turned out to be adjusting spring constant. While many jobs were successfully converged by one or a few attempts of tightening the spring constant, several resilient jobs went through multi-step parameter adjustments. An example is mace-mp shown in Table 2 where agent chose to increase the spring constant twice consecutively, i.e.  $0.3 \rightarrow 0.5 \rightarrow 1.2$ , then increased the NEB image size by 2 from 13. Finally, agent decreased the spring constant from  $1.2 \rightarrow 0.5$  and successfully achieved the energy convergence. Token usage averaged approximately 1,600 per retry, with communication times ranging from 6 to 14 seconds, signifying sound throughput performance across the DOE leadership computing facilities.

AI-driven workflow automation can also validate the robustness of scientific discoveries. Table 3 shows the sensitivity of MLIP prediction by adjusting a convergence criterion; the maximum force between  $0.1 - 0.3$  eV/Å. While the mean is an important indicator to select a suitable surrogate out of dozen of very powerful pretrained MLIP models currently available, highly accurate model prediction does not warrant its robustness [12]. The distribution of the model predictions helps researchers to systematically select a set MLIP models suitable for microkinetics study.

**Table 3: Sensitivity of activation energy with NEB parameters**

MLIP	mean	min	max	stdev
allegro-mp-l	3.3425	3.3064	3.5144	0.0615
allegro-oam-l	3.0453	2.812	3.1303	0.1226
dpa2	2.2842	2.1733	2.5763	0.1145
dpa3	2.5555	2.5128	2.5982	0.0438
equiformer-v3	2.153	2.1523	2.1543	0.0008
mace-mp	2.0936	1.9454	2.146	0.0529
mace-omat	1.7949	1.7676	2.0726	0.0667
matris-oam	2.9847	2.8798	3.3752	0.1337
nequip-mp-l	1.476	1.3604	2.0854	0.1602
nequip-oam-l	2.2994	2.2158	2.6137	0.0895
nequip-oam-m	2.4265	2.4244	2.431	0.0018
pet-omat	2.0713	2.047	2.2021	0.0535

## 4 Conclusion

We have developed a portable and scalable AI skill that automates NEB calculations by combining agentic reasoning, HPC, and universal MLIPs. Beyond reducing manual intervention, our study demonstrates how domain expertise can be encapsulated into reusable AI skills that autonomously recover from failures, benchmark competing surrogate models, and quantify the robustness of scientific predictions. AI automation also facilitate uncertainty quantification; a critical step for reliable and reproducible science. As scientific foundation models and HPC resources continue to grow, collections of interoperable AI skills executed across distributed computing facilities could form the basis of autonomous scientific campaigns capable of accelerating materials discovery in the era of exascale computing and beyond.

## Acknowledgments

The authors acknowledge support from the ARO cooperative agreement W911NF-25-2-0183. This research used computing resources under Innovative and Novel Computational Impact on Theory and Experiment (INCITE) at the Argonne Leadership Computing Facility. This research also used resources of the National Energy Research Scientific Computing Center (NERSC), a Department of Energy User Facility using NERSC award BES-ERCAP 0035639. This work used computational resources of Hokusai provided by RIKEN through the HPCI System Research Project (Project ID: hp260089).

## References

- [1] Agent Skills Working Group. 2026. Agent skills specification: portable ai agent expertise via skill.md. The official standard for progressive-disclosure procedural capabilities across AI coding agents. Retrieved June 18, 2026 from <https://agentskills.io>.
- [2] Anthropic and Agentic AI Foundation. 2024. Model context protocol (mcp): an open standard for integrating ai models with external tools and data. Maintained by the Agentic AI Foundation under the Linux Foundation. Retrieved June 18, 2026 from <https://modelcontextprotocol.io>.
- [3] Ilyes Batatia, Simon Batzner, Dávid P. Kovács, Albert Musaelian, Gregor N. C. Simm, Ralf Drautz, Christoph Ortner, Boris Kozinsky, and Gábor Csányi. 2025. The design space of  $E(3)$ -equivariant atom-centred interatomic potentials. *Nature Machine Intelligence*, 7, 1, 56–67. doi:10.1038/s42256-024-00956-x.
- [4] Ilyes Batatia, Dávid Péter Kovács, Gregor N. C. Simm, Christoph Ortner, and Gábor Csányi. 2022. MACE: Higher Order Equivariant Message Passing Neural Networks for Fast and Accurate Force Fields. In *Advances in Neural Information Processing Systems*. Vol. 35, 11423–11436.

- [5] Simon Batzner, Albert Musaelian, Lixin Sun, Mario Geiger, Jonathan P. Mailoa, Mordechai Kornbluth, Nicola Molinari, Tess E. Smidt, and Boris Kozinsky. 2022. E(3)-Equivariant Graph Neural Networks for Data-Efficient and Accurate Interatomic Potentials. *Nature Communications*, 13, 2453. doi:10.1038/s41467-022-29939-5.
- [6] Peter E. Blöchl. 1994. Projector augmented-wave method. *Physical Review B*, 50, (Dec. 1994), 17953–17979, 24, (Dec. 1994). doi:10.1103/PhysRevB.50.17953.
- [7] Daniil A. Boiko, Robert MacKnight, Ben Kline, and Gabe Gomes. 2023. Autonomous chemical research with large language models. *Nature*, 624, 7992, (Dec. 2023), 570–578. doi:10.1038/s41586-023-06792-0.
- [8] Roberto Car and Michele Parrinello. 1985. Unified approach for molecular dynamics and density-functional theory. *Physical Review Letters*, 55, (Nov. 1985), 2471–2474, 22, (Nov. 1985). doi:10.1103/PhysRevLett.55.2471.
- [9] William Dawson, Louis Beal, Yoann Curé, Giuseppe Fiscaro, Dorian Rolland, and Luigi Genovese. 2026. Lara: validation-driven agentic supercomputer workflows for atomistic modeling. *arXiv:2604.22571*.
- [10] Ralf Drautz. 2019. Atomic cluster expansion for accurate and transferable interatomic potentials. *Physical Review B*, 99, 1, (Jan. 2019), 014104. doi:10.1103/PhysRevB.99.014104.
- [11] Abhimanyu Dubey et al. 2024. The llama 3 herd of models. *arXiv preprint arXiv:2407.21783*. <https://arxiv.org/abs/2407.21783> arXiv: 2407.21783 [cs.LG].
- [12] Xiang Fu, Zhenghao Wu, Wujie Wang, Tian Xie, Sinan Keten, Rafael Gomez-Bombarelli, and Tommi Jaakkola. 2023. Forces are not enough: benchmark and critical evaluation for machine learning force fields with molecular simulations. *Transactions on Machine Learning Research*. arXiv: 2210.07237 [physics.comp-ph]. doi:10.48550/arXiv.2210.07237.
- [13] Shanghua Gao et al. 2025. Democratizing ai scientists using tooluniverse. *arXiv:2509.23426*.
- [14] Gemma Team et al. 2024. Gemma: open models based on gemini research. *arXiv preprint arXiv:2403.08295*. <https://arxiv.org/abs/2403.08295> arXiv: 2403.08295.
- [15] Stefan Grimme. 2004. Accurate description of van der waals complexes by density functional theory including empirical corrections. *Journal of Computational Chemistry*, 25, 12, 1463–1473. doi:https://doi.org/10.1002/jcc.20078.
- [16] Yikang Han, Ai Liu, and Haihao Wang. 2023. A survey of vector databases in the era of large language models. *arXiv preprint arXiv:2310.11703*. Standard survey for modern vector database architectures.
- [17] Shinnosuke Hattori, Kohei Shimamura, Aiichiro Nakano, Rajiv K. Kalia, Priya Vashishta, and Ken-ichi Nomura. 2025. Beyond scaling: chemical intuition as emergent ability of universal machine learning interatomic potentials. (June 2025). arXiv: 2506.07579 [cond-mat.mtrl-sci]. <https://arxiv.org/abs/2506.07579>.
- [18] Graeme Henkelman, Blas P. Uberuaga, and Hannes Jónsson. 2000. A climbing image nudged elastic band method for finding saddle points and minimum energy paths. *The Journal of Chemical Physics*, 113, 22, 9901–9904. doi:10.1063/1.1329672.
- [19] Pierre Hohenberg and Walter Kohn. 1964. Inhomogeneous electron gas. *Physical Review*, 136, (Nov. 1964), B864–B871, 3B, (Nov. 1964). doi:10.1103/PhysRev.136.B864.
- [20] Kelly Hong, Anton Troynikov, and Jeff Huber. 2025. Context Rot: How Increasing Input Tokens Impacts LLM Performance. Tech. rep. Comprehensive empirical study mapping performance cliffs across 18 frontier long-context language models. Chroma, (July 2025). <https://research.trychroma.com/context-rot>.
- [21] Hannes Jónsson, Greg Mills, and Karsten W. Jacobsen. 1998. Nudged elastic band method for finding minimum energy paths of transitions. In *Classical and Quantum Dynamics in Condensed Phase Simulations*. Bruce J. Berne, Giovanni Cicotti, and David F. Coker, (Eds.) The original seminal paper formulating the standard NEB algorithm. World Scientific, 385–404.
- [22] Colonel Vijay Kumar and Balasubramanian Kandasubramanian. 2019. Advances in ablative composites of carbon based materials: a review. *Industrial & Engineering Chemistry Research*, 58, 51, 22663–22701. eprint: <https://doi.org/10.1021/acs.iecr.9b04625>. doi:10.1021/acs.iecr.9b04625.
- [23] Rosanna Larciprete, Stefano Fabris, Tao Sun, Paolo Lacovig, Alessandro Baraldi, and Silvano Lizzit. 2011. Dual path mechanism in the thermal reduction of graphene oxide. *Journal of the American Chemical Society*, 133, 43, 17315–17321. PMID: 21846143. eprint: <https://doi.org/10.1021/ja205168x>. doi:10.1021/ja205168x.
- [24] Chris Lu, Cong Lu, Robert Tjarko Lange, Yutaro Yamada, Shengran Hu, Jakob Foerster, David Ha, and Jeff Clune. 2026. Towards end-to-end automation of ai research. *Nature*, 651, 8107, (Mar. 2026), 914–919. doi:10.1038/s41586-026-1026-5-5.
- [25] Andres M. Bran, Sam Cox, Oliver Schilter, Carlo Baldassari, Andrew D. White, and Philippe Schwaller. 2024. Augmenting large language models with chemistry tools. *Nat. Mach. Intell.*, 6, 5, (May 2024), 525–535. doi:10.1038/s42256-024-00832-8.
- [26] Robert MacKnight, Daniil A. Boiko, Jose Emilio Regio, Liliana C. Gallegos, Théo A. Neukomm, and Gabe Gomes. 2025. Rethinking chemical research in the age of large language models. *Nat. Comput. Sci.*, 5, 9, (Sept. 2025), 715–726. doi:10.1038/s43588-025-00811-y.
- [27] Christopher D. Manning, Prabhakar tug Raghavan, and Hinrich Schütze. 2008. *Introduction to Information Retrieval*. Cambridge University Press, New York. ISBN: 0521865719.
- [28] Albert Musaelian, Simon Batzner, Anders Johansson, Lixin Sun, Cameron J. Owen, Mordechai Kornbluth, and Boris Kozinsky. 2023. Learning local equivariant representations for large-scale atomistic dynamics. *Nature Communications*, 14, 579. doi:10.1038/s41467-023-36329-y.
- [29] NobelPrize.org. 2026. The Nobel Prize in Chemistry 2013. Retrieved Jun 25, 2026 from <https://www.nobelprize.org/prizes/chemistry/2013/summary>.
- [30] [SW] Ken-ichi Nomura, nebskill: Nudged Elastic Band software utilities and analysis tools 2026. URL: <https://github.com/KenichiNomura/nebskill>.
- [31] [SW] NVIDIA Corporation, NVIDIA NemoClaw: Enterprise-Grade Agent Orchestration and Security Stack 2026. URL: <https://blogs.nvidia.com/blog/industry-software-leaders-secure-autonomous-ai-engineers-nemoclaws/>.
- [32] OpenAI. 2025. Gpt-oss: open-weight language models with advanced reasoning and tool use capabilities. <https://github.com/openai/gpt-oss>. (2025).
- [33] Michael C. Payne, Michael P. Teter, Douglas C. Allan, Tomás. A. Arias, and John D. Joannopoulos. 1992. Iterative minimization techniques for ab initio total-energy calculations: molecular dynamics and conjugate gradients. *Reviews of Modern Physics*, 64, (Oct. 1992), 1045–1097, 4, (Oct. 1992). doi:10.1103/RevModPhys.64.1045.
- [34] John P. Perdew, Kieron Burke, and Matthias Ernzerhof. 1996. Generalized gradient approximation made simple. *Physical Review Letters*, 77, (Oct. 1996), 3865–3868, 18, (Oct. 1996). doi:10.1103/PhysRevLett.77.3865.
- [35] Edward O. Pyzer-Knapp, Jed W. Pitera, Peter W. J. Staar, Seiji Takeda, Teodoro Laino, Daniel P. Sanders, James Sexton, John R. Smith, and Alessandro Curioni. 2022. Accelerating materials discovery using artificial intelligence, high performance computing and robotics. *npj Computational Materials*, 8, 1, (Apr. 2022), 84. doi:10.1038/s41524-022-00765-z.
- [36] Taufeq Mohammed Razakh et al. 2025. Multiscale light-matter dynamics in quantum materials: from electrons to topological superlattices. In *Proceedings of the International Conference for High Performance Computing, Networking, Storage and Analysis (SC '25)*. Association for Computing Machinery, 36–47. doi:10.1145/3712285.3771785.
- [37] Janosh Riebesell et al. 2023. Matbench Discovery – a framework to evaluate machine learning crystal stability predictions. *arXiv preprint arXiv:2308.14920*, (Aug. 2023). arXiv: 2308.14920 [cond-mat.mtrl-sci]. doi:10.48550/arXiv.2308.14920.
- [38] Fuyuki Shimojo et al. 2019. Qxmd: an open-source program for nonadiabatic quantum molecular dynamics. *SoftwareX*, 10, 100307. doi:https://doi.org/10.1016/j.softx.2019.100307.
- [39] [SW] Peter Steinberger and The OpenClaw Foundation, OpenClaw: An Open-Source Autonomous AI Agent Framework 2026. URL: <https://github.com/OpenClaw/openclaw>.
- [40] Tao Sun, Stefano Fabris, and Stefano Baroni. 2011. Surface precursors and reaction mechanisms for the thermal reduction of graphene basal surfaces oxidized by atomic oxygen. *The Journal of Physical Chemistry C*, 115, 11, 4730–4737. eprint: <https://doi.org/10.1021/jp111372k>. doi:10.1021/jp111372k.
- [41] Hiroshi Takemiya, Yoshio Tanaka, Satoshi Sekiguchi, Shuji Ogata, Rajiv K. Kalia, Aiichiro Nakano, and Priya Vashishta. 2006. Sustainable adaptive grid supercomputing: multiscale simulation of semiconductor processing across the pacific. In *SC '06: Proceedings of the 2006 ACM/IEEE Conference on Supercomputing*, 23–23. doi:10.1109/SC.2006.59.
- [42] [SW] Vercel Labs and The Agent Skills Directory Contributors, The Agent Skills Directory and CLI (skills.sh) 2026. URL: <https://www.skills.sh>.
- [43] Ziqi Wang, Hongshuo Huang, Hancheng Zhao, Changwen Xu, Shang Zhu, Jan Janssen, and Venkatasubramanian Viswanathan. 2025. Dreams: density functional theory based research engine for agentic materials simulation. *arXiv:2507.14267*.
- [44] Shunyu Yao, Jeffrey Zhao, Dian Yu, Nan Du, Izhak prestige Shafran, Karthik R. Narasimhan, and Yuan Cao. 2023. ReAct: synergizing reasoning and acting in language models. In *International Conference on Learning Representations (ICLR)*. OpenReview.net. [https://openreview.net/forum?id=WE\\_vluYUL-X](https://openreview.net/forum?id=WE_vluYUL-X).
- [45] Jian Zhao et al. 2026. High-temperature memristors enabled by interfacial engineering. *Science*, 392, 6799, 771–779. eprint: <https://www.science.org/doi/pdf/10.1126/science.aeb9934>. doi:10.1126/science.aeb9934.